

Novel Photosensitizers for the *E/Z*-Isomerization of Trienes.¹ Part 2.² Mechanistic and Photophysical Aspects

Karl-Heinz Pfoertner* and Manfred Voelker

Central Research Units, F. Hoffmann-La Roche Ltd, Basle, Switzerland

To investigate the reaction mechanism, the disodium salts of *o*-(6-hydroxy-3-oxo-3*H*-xanthen-9-yl)benzenesulphonic acid and its thioxanthene analogue were selected from a class of photosensitizers firstly applied to the *E/Z*-isomerization of trienes. As an example of the latter the conversion of tachysterol into previtamin D was chosen. A presentation of the photophysical properties of six sensitizers with xanthene, thioxanthene and selenoxanthene moieties and a description of the aggregation phenomena of the above-mentioned two compounds completes this study.

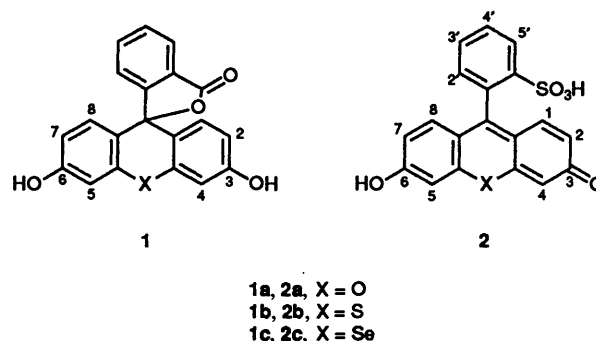
The preceding paper² is concerned with a novel class of photosensitizers for the *E/Z*-isomerization of trienes, and its synthesis and application to the technically useful conversion to tachysterol (T) into pre-vitamin D (P) and to the same reaction with their 1 α ,25-dihydroxy analogues. We now consider the appropriate mechanistic and photophysical aspects. Snoeren *et al.*³ reported that fluoren-9-one photosensitizes the transformation of tachysterol trimethyl silyl ether into the corresponding previtamin D derivative.

Surprisingly, in this reaction anthracene was found to be completely ineffective as a sensitizer,³ though the energy of its first excited triplet state (178.8 kJ mol⁻¹) is not far from the triplet energy of T which, by Denny and Liu,⁴ was estimated to be in the range 192–200 kJ mol⁻¹. Indeed, for the synthesis of vitamin D (D) Stevens⁵ previously claimed the anthracene photosensitized conversion of T into P within a double-irradiation procedure analogous to that described by Eyley and Williams.⁶

In order to find out the reason for this discrepancy^{3,5} we performed molecular-modelling studies concerning the *E/Z*-isomerization of the four possible rotamers of T (*tEc*, *cEc*, *tEt* and *cEt*)⁷ in comparison with the rotamers of the corresponding trimethylsilyl ether. The latter also exhibited no steric hindrance in this reaction. The molecular modelling studies only support the assumption⁸ that the *tEc* rotamer predominates in the conformational equilibrium.

At a concentration of 1.6×10^{-4} mol dm⁻³ anthracene is an effective photosensitizer⁵ for the (*E/Z*)-isomerization of T, whereas Snoeren *et al.*³ using an anthracene concentration of 0.17 mol dm⁻³, found that no reaction occurred. Thus, the role of the anthracene concentration is striking. Since anthracene concentrations ≥ 0.1 mol dm⁻³ are recommended for the photochemical preparation of dianthracene,⁹ in this concentration range its photosensitization properties are evidently suppressed by self-quenching.¹⁰ Complete elimination of anthracene from the reaction mixture can be achieved only by column chromatography, but this method is not feasible for the production of P on a large scale. To overcome this difficulty Slemon¹¹ has developed liquid polymer-bound anthracene sensitizers which, after the photochemical reconversion of T into P, are precipitated as an oil by adding MeOH to the reaction mixture. Because the starting material 7-dehydrocholesterol (7-DHC) is also sparingly soluble in MeOH, it would be precipitated together with the polymer-bound anthracene, provided that the remaining 7-DHC exceeds 6–7%. As has already been mentioned,² for practical purposes the irradiation of 7-DHC is stopped at conversion rates < 50%. After having performed the second irradiation in the presence of a photosensitizer, the remaining 7-DHC is then precipitated by

MeOH and can only be recycled directly when it is not contaminated with a sensitizer. Therefore, novel photosensitizers for the (*E/Z*)-isomerization of T have been developed which can be separated from the reaction mixture by extraction with water. These sensitizers are disodium salts (**1a**₁–**c**₁) and (**2a**₁–**c**₁) which can be derived from the lactone **1** and from the benzenesulphonic acid **2**, respectively.²



Results and Discussion

Due to the increasing nuclear charge of X a bathochromic shift of the absorption maxima is observed in the benzoic acid series as well as in the benzenesulphonic acid series (Table 1). This shift is accompanied by an increase of the maximal absorption which reflects an enlargement of the optical cross section when proceeding in the order X = O, S, Se.

From the bathochromic shift of the fluorescence maxima with respect to the corresponding absorption maxima of the sensitizers considered (Stokes shift) the energies of their first excited singlet states have been calculated (Table 1). Though the energy differences are small, the tendency to decrease with increasing size of X is evident. In contrast with the singlet energies the triplet energies calculated from the phosphorescence onset are almost equal. Whereas the fluorescence emission decreased with increasing size of X, the phosphorescence intensities revealed the opposite behaviour, thus indicating an increase of the intersystem crossing (ISC) as a consequence of the internal heavy atom effect. Responsible for this effect is the spin-orbit interaction of the electrons which depends on the magnitude of the nuclear charge of X. Its increase leads to the appearance of usually forbidden singlet-triplet transitions by inverting the electron spin. The result is a decrease in the fluorescence intensity, since the first excited singlet state will be partly depopulated in favour of the lowest triplet state leading to an increase of the phosphorescence intensity. According to

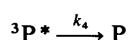
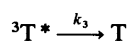
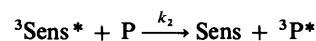
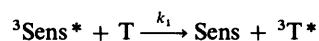
Table 1 Photophysical properties of the sensitizers **1a₁-c₁** and **2a₁-c₁**

| Sensitizer ^a | Absorption | | Fluorescence ^b λ _{max} /nm | Singlet-energy ^c E _s /kJ mol ⁻¹ | Phosphorescence ^d | | Triplet-energy E _T /kJ mol ⁻¹ |
|-------------------------|----------------------|--|---|---|------------------------------|------------------------|--|
| | λ _{max} /nm | ε/dm ³ mol ⁻¹ cm ⁻¹ | | | λ _{max} /nm | λ _{onset} /nm | |
| 1a₁ | 495 | 26 800 | 520 | 236 ± 4 | 629 | 615 | 194 ± 3 |
| 1b₁ | 522 | 30 600 | 544 | 224 | 639 | 604 | 198 |
| 1c₁ | 530 | 55 500 | 550 | 222 | 652 | 613 | 195 |
| 2a₁ | 500 | 28 700 | 523 | 234 | 635 | 616 | 194 |
| 2b₁ | 530 | 35 400 | 548 | 222 | 653 | 620 | 193 |
| 2c₁ | 538 | 47 600 | 552 | 219 | 668 | 625 | 191 |

^a Prepared by adding 2 equiv. MeONa to EtOH solutions of **1a-c** and **2a-c**, respectively. ^b At room temperature. ^c The singlet-energies were calculated from 0.5 Stokes shift. ^d At 77 K.

the fact that the ratio of the nuclear charges of O, S and Se is *ca.* 1:2:4, the increasing ISC can also be recognized by the correspondingly shortened irradiation time which is necessary for reaching the photostationary state in the *E/Z*-isomerization of T when this reaction is sensitized by **1a₁-c₁** and **2a₁-c₁**, respectively.²

Based on the facts (a) that the conversion of T is significantly accelerated with increasing sensitizer ISC² and (b) that the novel sensitizers produce singlet oxygen,* we assume that the photosensitized *E/Z*-isomerization of the *E*-triene T proceeds *via* triplet-energy transfer. This is the starting point for the following theoretical treatment Sens = photosensitizer, P = *Z*-triene, T = *E*-triene provided that other types of deactivation than those considered here are negligible.



Then the photostationary state is characterized by eqns. (1) and (2).

$$k_1[{}^3\text{Sens}^*][\text{T}] = k_3[{}^3\text{T}^*] \quad (1)$$

$$k_2[{}^3\text{Sens}^*][\text{P}] = k_4[{}^3\text{P}^*] \quad (2)$$

In the photostationary state the ratio of the isomers P and T is given by multiplication of the ratio k_1/k_2 of the excitation rates by the ratio k_4/k_3 of the decay rates, eqn. (3).

$$\frac{[\text{P}]}{[\text{T}]} = \frac{k_1 k_4 [{}^3\text{P}^*]}{k_2 k_3 [{}^3\text{T}^*]} \quad (3)$$

The small difference in the energies of ${}^3\text{T}^*$ and ${}^3\text{P}^*$ allows the approximation $[{}^3\text{P}^*]/[{}^3\text{T}^*] \approx 1$ from which eqn. (4) is derived.

$$\frac{[\text{P}]}{[\text{T}]} = \frac{k_1 k_4}{k_2 k_3} \quad (4)$$

* Demonstrated by the photooxygenation of 2,3-dimethylbut-2-ene to 3-hydroperoxy-2,3-dimethylbut-1-ene analogous to the procedure of Foote and Uhde.¹⁹

With 194.2 kJ mol⁻¹ the average triplet energy of our sensitizers (Table 1) lies within the range 192–200 kJ mol⁻¹ estimated⁴ for the triplet energies of P and T. In this case diffusion-controlled energy transfer to the *E*-triene T is still possible, but not to the *Z*-triene P, *i.e.* $k_1 > k_2$.

The *E*-triene triplet decomposes *via* a phantom triplet leading to the ground state *E*- and *Z*-trienes T and P in about equal portions.

Because the *Z*-triene P will not be excited to the same extent, the *E*-triene will be largely pumped into the *Z*-state. In other words, since the triplet energies of our sensitizers lie within the range of the triplet energies of the *E*- and *Z*-trienes, the *E/Z*-ratio will be determined by the ratio of the excitation rates k_1/k_2 , whereas with sensitizers of high triplet energies such as fluoren-9-one the *E/Z*-ratio will be determined by the ratio k_4/k_3 of the decay rates.

Depending on dye concentration, solvent and temperature, xanthene dyes form aggregates, preferably dimers but also trimers and higher aggregates.¹² Since the formation of aggregates modifies the photophysical properties of a dye, it affects its ability to act as a photosensitizer. Spectral shifts, non-conformity with Beer's law, and fluorescence quenching at high concentrations are all indicative of aggregation phenomena. This was shown by Arbeloa¹³⁻¹⁵ as well as by Xu and Neckers¹⁶ who studied, in different solvents, the dianionic forms of fluorescein and Rose Bengal, respectively.

In general, dyes aggregate more strongly in water than in organic solvents. The *E/Z*-isomerizations of the *E*-triene tachysterol into the *Z*-triene previtamin D² already described were performed by applying relatively high sensitizer concentrations of 3×10^{-4} mol dm⁻³ using organic solvents. Nevertheless, we suggest that dimers and possibly higher aggregates were present. Values for dimer triplet energies of xanthenes have been reported by Chambers and Kearns.¹⁷ These data indicate that the triplet energies of dimeric aggregates are *ca.* 5 kJ mol⁻¹ lower than those of the corresponding monomers.

For the investigation of aggregation phenomena we chose the sensitizers **2a₁** and **2b₁** dissolved in 0.1 mol dm⁻³ NaOH and we began with measurements of their absorption spectra. Owing to the formation of dimers and possibly of higher aggregates the absorption spectra of both sensitizers are changed with increasing sensitizer concentration (Figs. 1 and 2).

According to Arbeloa's theoretical treatment of such problems¹⁴ we used our data to determine the monomer-dimer equilibria and to calculate absorption spectra of the sensitizer dimers. From the concentration-dependent absorption spectra of **2a₁** (Fig. 1) a dimerization constant $K = 20$ dm³ mol⁻¹ defined as $K = [\text{dimer}]/[\text{monomer}]^2$ was calculated for the concentration range up to 4×10^{-3} mol dm⁻³. The corresponding spectra of **2b₁** (Fig. 2) led to a dimerization constant $K = 15$ dm³ mol⁻¹ for a concentration range up to 10^{-2} mol dm⁻³. At higher sensitizer concentrations the *K*-values increased

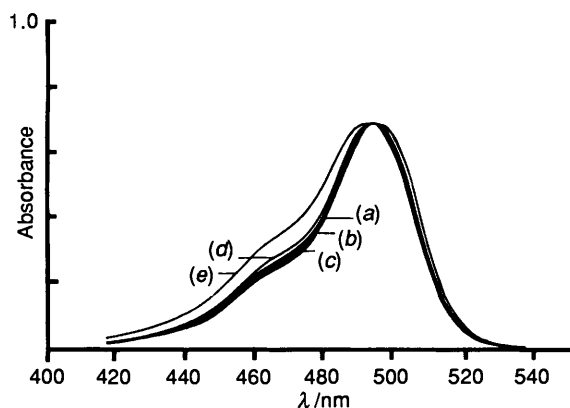


Fig. 1 Visible absorption spectra of the dianion $2a_1$, at different concentrations mol dm^{-3} in 0.1 mol dm^{-3} NaOH at 20°C , normalized to $\lambda = 496 \text{ nm}$: (a) 8.0×10^{-6} ; (b) 1.0×10^{-3} ; (c) 2.1×10^{-3} ; (d) 3.9×10^{-3} ; (e) 5.2×10^{-3} .

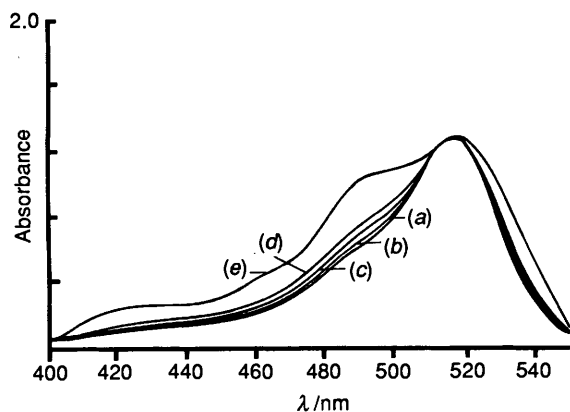


Fig. 2 Visible absorption spectra of the dianion $2b_1$, at different concentrations mol dm^{-3} in 0.1 mol dm^{-3} NaOH at 20°C , normalized to $\lambda = 518 \text{ nm}$: (a) 2.0×10^{-6} ; (b) 2.0×10^{-3} ; (c) 5.0×10^{-2} ; (d) 1.0×10^{-2} ; (e) 1.5×10^{-2} .

Table 2 Excitonic parameters for the dimers of $2a_1$ and $2b_1$ ^a

| Parameter | Dimeric $2a_1$ | Dimeric $2b_1$ |
|--------------------|----------------|----------------|
| M/D | 8.3 ± 0.3 | 7.9 ± 0.3 |
| U/cm^{-1} | 430 ± 25 | 820 ± 50 |
| $\theta/^\circ$ | 60 ± 2 | 51 ± 2 |
| $R_1/\text{\AA}$ | 7.4 ± 0.5 | 6.2 ± 0.5 |
| $R_2/\text{\AA}$ | 10.1 ± 0.5 | 7.7 ± 0.5 |

^a M = transition moment of the monomer; U = resonance interaction; θ = angle between polarization axes of the monomers; R_1 and R_2 represent the distances between the monomers in the dimers, model 1 and model 2, respectively.

dramatically. This is probably due to the formation of trimers and/or higher aggregates. Thus, the spectra (e) in Figs. 1 and 2 cannot be described by means of a dimeric aggregation but represent more complicated aggregation processes.

The dimerization constants obtained for $2a_1$ and $2b_1$ considerably exceed the value for uranine, reported by Arbeloa¹⁴ to be $K = 5 \text{ dm}^3 \text{ mol}^{-1}$. This seems to indicate that in our experiments stronger forces effect the cohesion of the sensitizer molecules than in Arbeloa's case. Since it is well known that in aqueous solution intermolecular hydrogen bonds are most important for the aggregation of uranine,²⁰ we conclude that the anions from the sulphonic acid groups of $2a_1$ and $2b_1$ contribute to more stable intermolecular hydrogen bonds than the anion of the carboxylic group of uranine. The

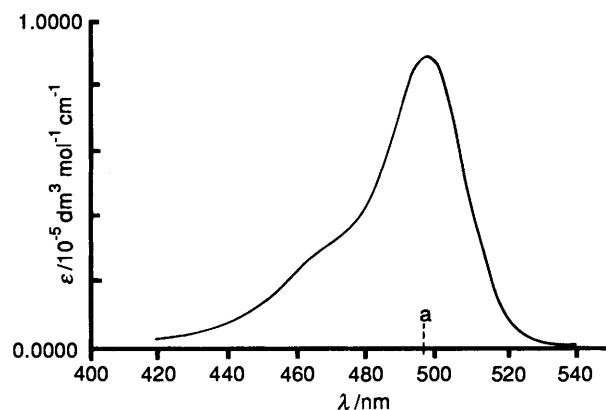
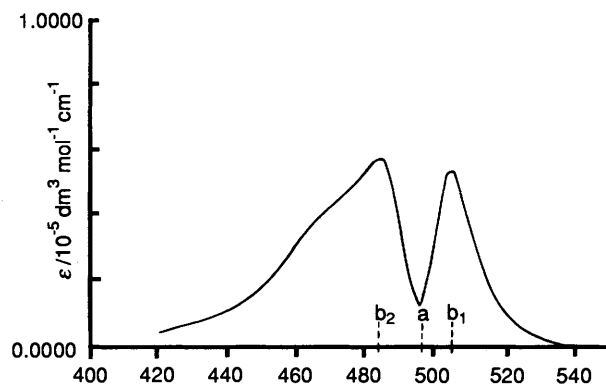


Fig. 3 Below: absorption spectrum for the $2a_1$ monomer with a maximum at $\lambda(a)$. Above: calculated absorption spectrum of the $2a_1$ dimer with two maxima at $\lambda(b_1)$ and $\lambda(b_2)$.

absorption spectrum of the monomer and the calculated spectra of the corresponding dimers derived from $2a_1$ and $2b_1$ are given in Figs. 3 and 4, respectively.

We recognized that both sensitizers reveal a strong band-splitting upon dimerization. Thus, according to exciton theory these dimers cannot be parallel or linearly arranged but must exhibit an intermediate geometry.^{12,18} From the separate monomer and dimer spectra the following excitonic parameters for the dimers of $2a_1$ and $2b_1$ could be elucidated (Table 2).

One must distinguish between two models.¹⁴ In model 1 the dimer-forming monomers are arranged in parallel planes but in model 2 they are arranged within the same plane. Intermolecular distances in the crystalline state are not known for our sensitizers and distances in solution can only roughly be estimated. For the uranine dimer (model 1) Arbeloa¹⁴ reports a monomer distance of 4.6 \AA . Assuming a similar orientation of our sensitizers we obtain a monomer distance of 7.4 \AA in the dimer derived from $2a_1$ and of 6.2 \AA in the dimer derived from $2b_1$. The larger intermolecular distance in the $2a_1$ dimer produces a much smaller resonance interaction U than in the $2b_1$ dimer (Table 2). The result is a weaker band splitting in the calculated spectrum of the $2a_1$ dimer (Fig. 3) compared with that of the $2b_1$ dimer (Fig. 4).

The formation of excimers also depends on the dye concentration. Excimers can be detected by their broad non-structured band in the fluorescence spectrum. When we performed the fluorescence measurements in a standard cuvette with a path length of 1 cm an increase in the sensitizer concentration led to a red shift of the corresponding emission maximum. This shift was in the order of magnitude of tens of nanometers and must be ascribed to the reabsorption of the short-wave emission of the fluorescence band. By reducing the optical path-length to *ca.* 10^{-3} cm and detecting the emitted

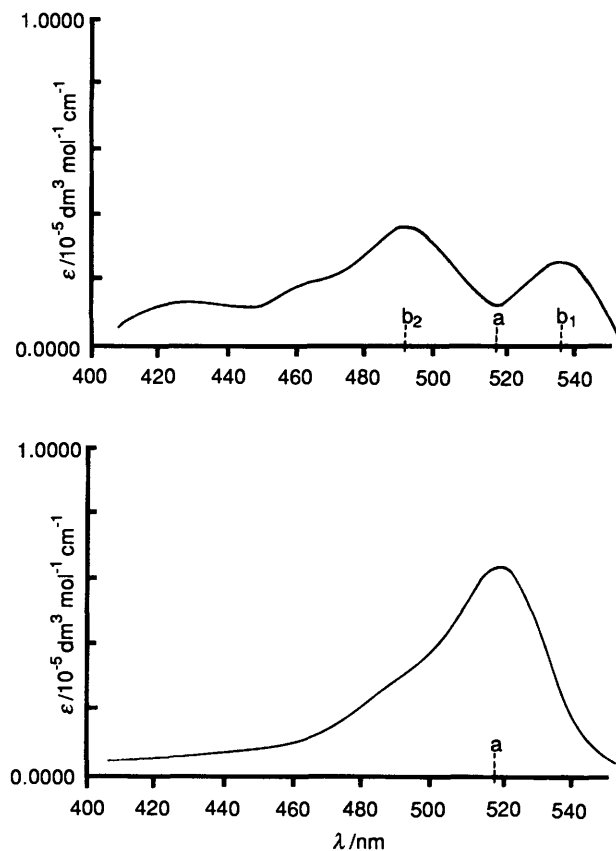


Fig. 4 Below: absorption spectrum for the $2b_1$ monomer with a maximum at $\lambda(a)$. Above: calculated absorption spectrum of the $2b_1$ dimer with two maxima at $\lambda(b_1)$ and $\lambda(b_2)$.

light on the site of the incident exciting light the reabsorption could be completely eliminated. In this case the emission spectra of the solutions with 2×10^{-2} and 2×10^{-6} mol dm $^{-3}$ sensitizer concentration became identical. By this way no excimer emission could be detected. Therefore, the formation of complexes in the excited states of $2a_1$ and $2b_1$ can be excluded.

Experimental

Determination of the photophysical data of the sensitizers $1a_1$ – c_1 and $2a_1$ – c_1 (Table 1) was achieved using solutions which were prepared by dissolving the respective compounds $1a$ – c and $2a$ – c with 2 equiv. sodium methoxide in ethanol (Uvasol, Merck). The concentration range for the light absorption measurements was 1×10^{-5} to 5×10^{-5} mol dm $^{-3}$ sensitizer, whereas the light emission measurements were performed in the lower concentration range of 1×10^{-6} to 1.4×10^{-5} mol dm $^{-3}$, in order to keep the absorbance of the excitation wavelengths < 0.1 . The optical pathlength was 1 cm. Experiments concerning the possible formation of sensitizer aggregates with respect to exciplexes were performed with 0.1 mol dm $^{-3}$ NaOH solutions in the sensitizer concentration range 2×10^{-6} to 2×10^{-2} mol dm $^{-3}$. Here the absorbance was kept constant by

corresponding variation of the optical path length. The absorption spectra were recorded on a Perkin-Elmer Lambda 9 with Data Station 3600 at 20 °C applying a 2 nm optical band width and a scan speed of 120 nm min $^{-1}$. Using a Perkin-Elmer LS 5 also combined with the Data Station 3600, the emission spectra were recorded at 20 °C with an optical bandwidth of 5 nm and a scan speed of 240 nm min $^{-1}$. If necessary, they were corrected by subtracting the emission spectra of the solvents.

The phosphorescence measurements were performed by means of a Perkin-Elmer low temperature luminescence accessory at ca. 77 K applying an optical path length of 2 mm.

The luminescence of some of the photosensitizers investigated was very weak. For this reason the fluorescence spectra of $1c_1$ and $2c_1$ and the phosphorescence spectra of $1a_1$ and $1b_1$ were measured repetitively. Averaging of 25 single measurements led in all cases to an adequate signal-to-noise ratio. Demonstration that these emission spectra were invariant to changes in wavelength of the exciting light confirmed their authenticity.

Acknowledgements

The authors thank Miss J. Stebler and Mr. A. Ritter for technical assistance and are particularly indebted to Dr. K. Müller for performing the molecular-modelling studies.

References

- 1 K. H. Pfoertner, presented in part at the VIth Chinese Symposium on Photochemistry, Beijing, 1989.
- 2 Part 1, preceding paper.
- 3 A. E. C. Snoeren, M. R. Daha, J. Lugtenburg and E. Havinga, *Recl. Trav. Chim. Pays-Bas*, 1970, **89**, 261.
- 4 M. Denny and R. S. Liu, *Nouv. J. Chim.*, 1978, **2**, 637.
- 5 USP 4 686 023/1987.
- 6 S. C. Eyley and D. H. Williams, *J. Chem. Soc., Chem. Commun.*, 1975, 858.
- 7 H. J. C. Jacobs and E. Havinga in *Advances in Photochemistry*, Wiley, Chichester, 1979, vol. 11, p. 305.
- 8 J. Lugtenburg and E. Havinga, *Tetrahedron Lett.*, 1969, 2391.
- 9 Houben-Weyl, *Methoden der Organischen Chemie*, ed. E. Müller, vol. IV, part 5a (Photochemie, Part 1), Thieme, Stuttgart, 1975, p. 479.
- 10 T. Förster, *Fluoreszenz Organischer Verbindungen*, Vandenhoeck & Ruprecht, Göttingen, 1982, p. 231.
- 11 EP 0 252 740/1988.
- 12 O. Valdes-Aguilera and D. C. Neckers, *Acc. Chem. Res.* 1989, **22**, 171 and literature cited therein.
- 13 L. Arbeloa, *J. Chem. Soc., Faraday Trans.*, 1981, **77**, 1325.
- 14 L. Arbeloa, *J. Chem. Soc., Faraday Trans.*, 1981, **77**, 1725.
- 15 L. Arbeloa, *J. Photochem.*, 1982, **18**, 161.
- 16 D. Xu and D. Neckers, *J. Photochem. Photobiol., A*, 1987, **40**, 361.
- 17 R. W. Chambers and D. R. Kearns, *J. Phys. Chem.*, 1968, **72**, 4718.
- 18 E. G. McRae and M. Kasha, *Physical Processes in Radiation Biology*, eds. L. Augenstein, B. Rosenberg, S. F. Mason, Academic Press, New York, 1963.
- 19 C. S. Foote and G. Uhde, *Organic Photochemical Syntheses*, eds. R. Srinivasan and T. D. Roberts, Wiley, New York, 1971, vol. 1, p. 60.
- 20 K. K. Rohatgi and A. K. Mukhophyay, *J. Indian Chem. Soc.*, 1972, **49**, 1311.

Paper 0/040501

Received 6th September 1990

Accepted 30th October 1990